Citation
Li, Z. and Chen, W. and Hao, H. 2019. Dynamic crushing and energy absorption of foam filled multi-layer folded structures: Experimental and numerical study. International Journal of Impact Engineering. 133: ARTN 103341. http://doi.org/10.1016/j.ijimpeng.2019.103341

Dynamic crushing and energy absorption of foam filled multi-layer folded structures: experimental and numerical study

Zhejian Li, Wensu Chen*, Hong Hao*

Centre for Infrastructural Monitoring and Protection
School of Civil and Mechanical Engineering, Curtin University, Australia

*corresponding author: wensu.chen@curtin.edu.au; hong.hao@curtin.edu.au

Abstract

Crushing behaviours of foam filled multi-layer truncated square pyramid (TSP) kirigami structures are studied experimentally and numerically in this study. Each layer of this TSP foldcore is folded using a single aluminium sheet with pre-cuts. Light weight foams are inserted into each unit cell of the TSP foldcore to enhance its loading and energy absorption capacity. The effects of the foam material, density and shapes of foam material on crushing resistance of the multi-layer folded structure are studied. Two foam materials, i.e. expanded polystyrene (EPS) foam with density of 13.5, 19 and 28 kg/m^3; rigid polyurethane (PU) foam with density of 35 kg/m^3 are used as foam infill for this multi-layer foldcore. Two shapes of PU foam infill are studied as well. Single layered TSP foldcores with foam infill are firstly studied under quasi-static crushing condition, then foam filled multi-layer TSP foldcores are crushed under dynamic loading conditions. Numerical models are verified with the experimental results, followed by intensive numerical simulations. Key parameters such as peak and average crushing resistance, densification strain and specific energy absorption are compared among the foldcores with different foam configurations. Comparing with other cellular structures, uniform collapsing of the proposed foldcore is observed under both quasi-static and dynamic loading conditions with the uniformity ratio ranging between 1.1 and 2.0. Significant increases

in average crushing resistances ranging from 36.6% to 82% are also observed by adding foam fillers, while the mass only increases by 3.2% to 20.4%.

Keywords: foam filled; dynamic crushing; foldcore; energy absorption

1. Introduction

Folded structures have been used widely as core of sandwich structures in recent years. The concept is to fold one or multiple sheets, unbroken or pre-cut, into certain geometries, and use these folded structures as core for sandwich structures. Miura type Origami structure as one of the most common folded structures have drawn much attention recently, due to its advantages such as continuous manufacturing and open channel design comparing with conventional sandwich core such as honeycomb [1]. However, due to its high initial peak stress, non-uniform collapsing [2] and high sensitivity to loading rate [1, 3], Miura-ori foldcore is less ideal for the application as energy absorbers. Plate buckling failure mode can be observed on Miura-ori foldcore under out-of-plane crushing, resulting in a high initial peak force followed by a drastic reduction in crushing resistance. Furthermore, it is not comparable to honeycomb structure in terms of crushing resistance [1]. Many other types of folded structures including stacked Miura-ori [4, 5], curved-crease origami foldcore [6, 7], kirigami structures [8, 9] and some other origami structures [10, 11] were developed to achieve a more uniform crushing behaviour throughout deformation with a lower initial peak force, which makes the structure more ideal for application as energy absorbers. Origami structures with tunable mechanical properties were developed as well [12, 13], where different mechanical properties such as stiffness can be observed at different stages of the deformation.

Truncated pyramid kirigami structures with different shapes and geometries were proposed in the previous studies [14, 15]. Superior energy absorption capability were demonstrated over many existing folded structures by yielding a high average crushing resistance, low initial peak

resistance and uniform collapsing of the foldcore under various loading conditions. The proposed foldcore also can be achieved by single sheet fabrication which is not feasible for some existing kirigami foldcores [8]. Blast mitigation capability of sacrificial cladding with this folded structure was investigated in [16, 17], great reduction of peak transmitted force to protected structure is shown for the proposed truncated pyramid foldcores. Dynamic crushing tests of multi-layer sandwich panel with truncated square pyramid (TSP) folded structure as core were carried out recently [18]. Consistent crushing behaviour and excellent specific energy absorption were achieved. Furthermore, the multi-layer setup makes the face skin reusable by replacing the core after each load as no bonding is required between skins and core, unlike conventional composite structures [19]. Fabrication time and cost can be greatly reduced by using this non-bonding reusable set-up. Therefore, TSP folded structure has great potential for applications as energy absorbing structures, such as impact attenuators, blast sacrificial cladding, and vehicle crash box etc. However, the wall thickness of the TSP foldcore should be thin, as thicker sheet may cause difficulty in folding the core near the corners. To further increase the compressive strength and energy absorption of the folded structure, alternatives, such as foam infill should be used other than increasing the cell wall thickness.

As lightweight material has the ability to undergo large deformation at almost constant stress [19, 20], foam material including metallic and polymeric foams have been filled in composite structures to improve their crushing resistance and energy absorption [21, 22]. It was suggested that the increase in crushing strength and energy absorption of foam filled structures is much higher than that of foam filler itself [23-25], due to the interaction between the foam filler and cellular structure cell walls. The blast mitigation capacity of single-layer PU filled TSP foldcore cladding has been numerically investigated in the previous work as well, with promising performance demonstrated.

In this study, the dynamic crushing behaviour of foam-filled multi-layer TSP foldcore with different types of foams, material densities and foam filler shapes are investigated experimentally and numerically. Five foam filler configurations are considered: cubic expanded polystyrene (EPS) foam of three densities (13.5, 19, 28 kg/m^3), rigid polyurethane (PU) foam (35 kg/m^3) of two shapes. Quasi-static crushing tests of single layer foam-filled TSP foldcores were carried out, followed by dynamic crushing tests of multi-layer foam filled TSP foldcores. Numerical analysis of dynamic crushing of these foam filled multi-layer TSP foldcores was conducted as well. Key parameters including average crushing force, initial peak crushing force and specific energy absorption are selected as criteria to evaluate the crushing responses of these foam filled multi-layer TSP foldcores and compare with the samples without foam filler.

2. Geometric parameters, multi-layer setup and material properties

2.1 Truncated square pyramid foldcore and multi-layer set-up

The same dimensions of TSP foldcore are used as in the previous study [15]. The geometry of the TSP unit cell is constrained by its triangular interconnections connecting adjacent sidewalls as shown in Figure 1 (a). The geometric parameters shown in Figure 1Figure *2* (b) can be expressed by three governing parameters: top and bottom edge length, *b, a* and core height, *H* as in [15]. Three governing parameters, a=40 mm, b=20 mm and H=20 mm are kept throughout this study. The designed dimension for a four-unit cell TSP foldcore is 80x80x20mm. Each layer of the TSP foldcore is manually folded from a single pre-cut aluminium sheet (Al 1060) with the thickness of 0.26 mm. Multiple stacked sheets are cut by water jet cutting, and then manually folded into the designed shape. The relative density or volumetric density of the TSP foldcore without foam filler is around 2.7%, which is calculated

by the overall volume of aluminium sheet over the volume of the space (80x80x20 mm) it occupies. The density of the TSP foldcore without foam filler is 72.9 kg/m^3.

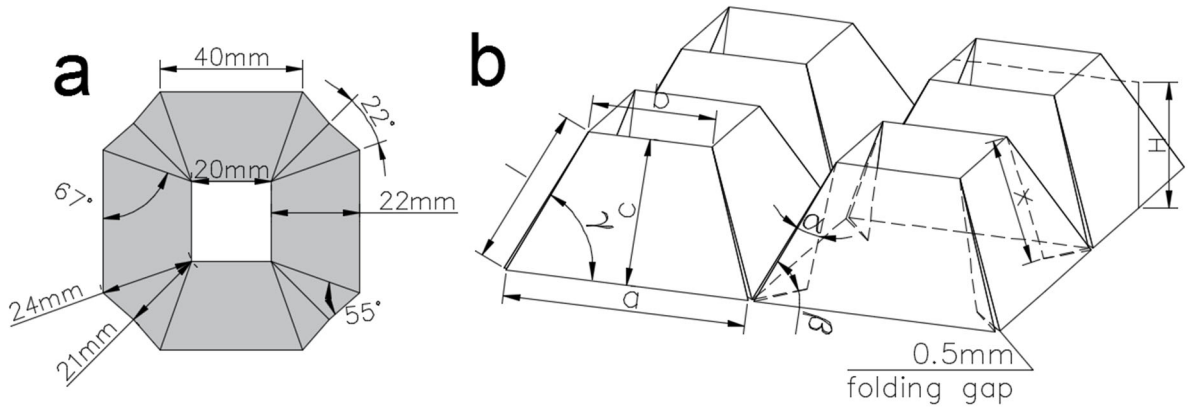

Figure 1. (a) Dimensions of a folding pattern of single unit cell; (b) Geometric parameters of TSP foldcore with four unit cells;

The reusable multi-layer set-up is shown in *Figure 2*. Each layer of TSP foldcore is separated by a 3 mm thick interlayer plate with drilled holes near corners. Each interlayer plate has a 2 mm high boundary in order to constrain the in-plane movement of outer sidewalls of the TSP foldcore under lateral deformation. Four threaded rods are then fastened on the base plate and pass through the holes of interlayer plates. These rods function as a movement guide for each layer under out-of-plane crushing of the structure. The holes on interlayer plates have a diameter of 8 mm, larger than the diameter of a M6 rod, therefore minimal interaction is expected between rods and interlayer plates during lateral movement. Neither glue nor other bonding is applied between foldcores and plates. After each test, the crushed core can be replaced with new specimen and the multi-layer set-up can be reused. The base plate and the interlayer plate are fabricated using aluminium alloy 5083, which has yield stress of 215 MPa and Young's Modulus of 71 GPa.

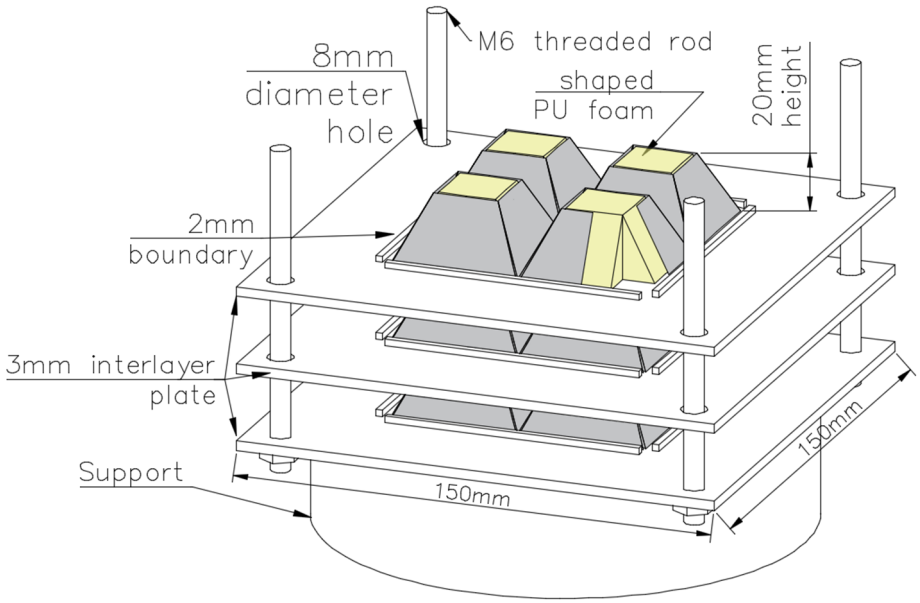

113

114 Figure 2. Reusable set-up of multi-layer shaped foam filled TSP foldcore

115 ## 2.2 Foam filler types

Foam filler configurations	Foam density (kg/m^3)	Foam shape	Foldcore mass (g)	Foam mass (g)	Increment in mass
TSP	-	-	9.3	-	-
TSP-EPS13.5C	13.5	Cubic	9.3	0.3	3.2%
TSP-EPS19C	19	Cubic	9.3	0.5	5.4%
TSP-EPS28C	28	Cubic	9.3	0.7	7.5%
TSP-PU35C	35	Cubic	9.3	0.9	9.7%
TSP-PU35S	35	Shaped	9.3	1.9	20.4%

116 Table 1. Foam configurations and mass of each layer (four unit cells)

117 Two types of foam materials i.e. expended polystyrene (EPS) and rigid polyurethane (PU) foam
118 are considered as foam filler. In total five foam filler configurations of foldcore are considered
119 in this study: TSP foldcore; TSP foldcore with cubic SL density grade (density of 13.5 kg/m^3)
120 EPS foam; TSP foldcore with cubic M density grade (density of 19 kg/m^3) EPS foam; TSP
121 foldcore with cubic VH density grade (density of 28 kg/m^3) EPS foam; TSP foldcore with cubic
122 PU foam (density of 35 kg/m^3); TSP foldcore with shaped PU foam (density of 35 kg/m^3). The
123 notation of the foam filler configuration includes foam type, foam density and foam shape. For

instance, TSP-EPS13.5C stands for TSP foldcore infilled with cubic EPS foam with density of 13.5 kg/m^3. Other notations and mass of each layer are listed in Table 1. The dimensions of two foam filler shapes and foam filler samples with four units each layer are shown in Figure 3.

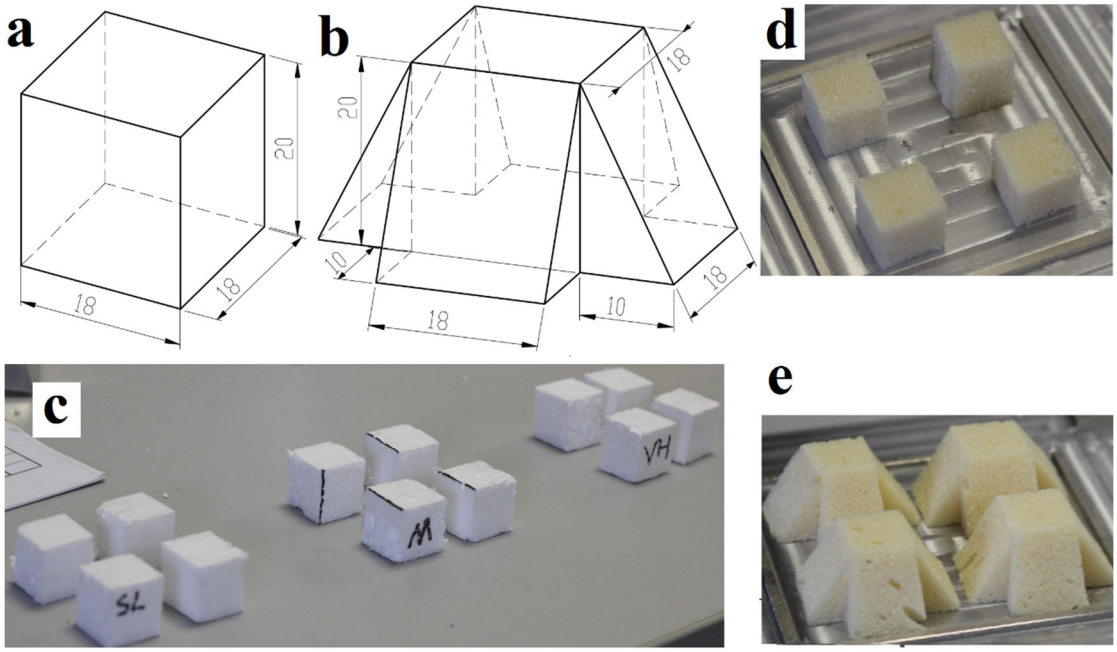

Figure 3. Dimensions of (a) cubic foam; (b) shaped foam; foam filler sample of (c) EPS cubic (with three densities); (d) PU cubic; (e) PU shaped

2.3 Material properties

Quasi-static tensile test of aluminium 1060 thin sheet used for foldcore preparation were carried out. A constant loading rate of 0.5 mm/min was applied to ensure a quasi-static loading condition as per the standard ASTM E8M-04 [26]. Two-dimensional direct image correlation (2D-DIC) technique was used for measuring the strain and displacement fields of specimens. Mechanical properties and true stress-strain data of the aluminium thin sheet used for foldcore preparation is given in Table 2 and presented in the previous study [16].

138

Parameter	Young's Modulus (GPa)		Poisson's ratio	Yield stress (MPa)		Density (kg/m^3)
Value	69		0.33	67.7		2710
True Strain	0	0.002	0.005	0.013	0.063	0.121
True Stress (MPa)	0	67.7	112.3	120.1	125.8	130.6

139 Table 2. Material properties and true stress-strain data of Aluminium 1060 *[16]*

140 Uniaxial compression tests of EPS19 and PU35 foams were carried out in this study under both
141 quasi-static and dynamic loading conditions. Properties of the other two types of foam material,
142 EPS13.5 and EPS28 are obtained from the previous study using the same setting and testing
143 machines [27]. The foam specimen with the diameter of 75 mm was used and three specimens
144 are tested for each case. Lloyd-Ametek EZ50 material testing machine was used for quasi-
145 static compression test applied with a constant loading rate of 1 mm/min. The dynamic
146 compressive tests of foam samples were carried out using INSTRON VHS 160/100-20 high
147 speed testing machine, which is designed to provide constant crushing velocity between 0.1 to
148 25 m/s. Crushing speed of 10 m/s was tested for both foam and foam filled multi-layer TSP
149 foldcores in the later sections. It is worth noting that the actual crushing speed is not constant
150 throughout dynamic crushing. More details of the dynamic test set-up and actual crushing
151 speed are provided in section 3.2. Photographs of dynamic crushing test on foams are shown
152 in Figure 4. Their engineering stress-strain curves under quasi-static and dynamic crushing
153 conditions are shown in Figure 5.

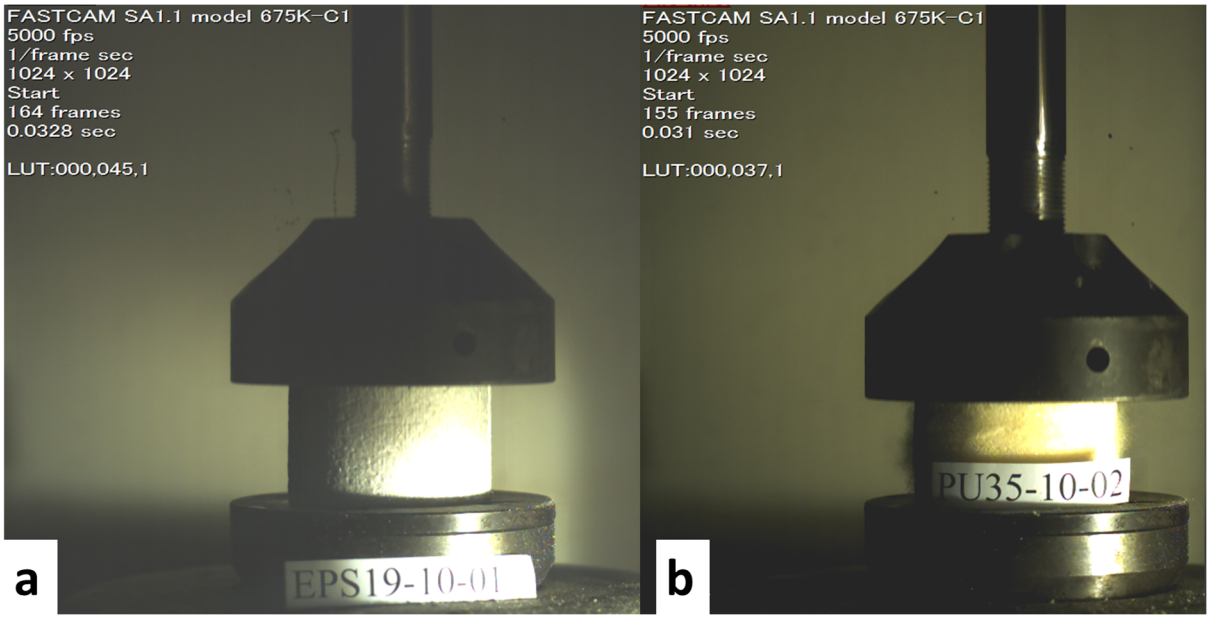

154

155 Figure 4. Dynamic compression test under 10m/s speed (a) EPS19; (a) PU35 foam

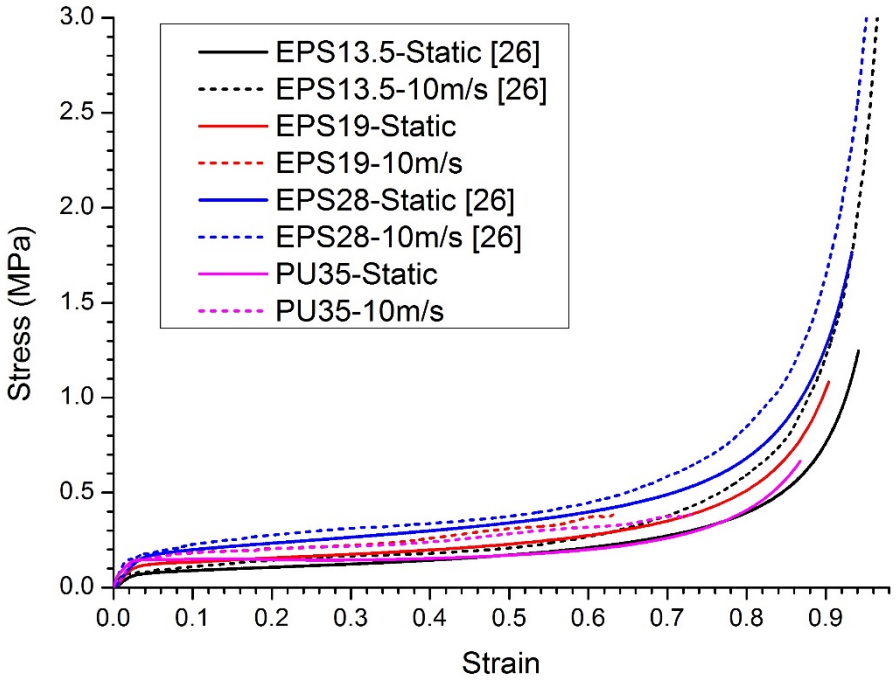

156

157 Figure 5. Engineering stress-strain curves of four foams under both quasi-static crushing and

158 10m/s dynamic crushing

3. Experimental analysis

3.1 Quasi-static crushing test

Single-layer crushing tests were conducted first for these five foam filler configurations. As found in the previous study [18], under quasi-static loading condition, the single-layer TSP foldcore shows similar overall crushing behaviour as the three-layer TSP foldcore. The average crushing force and the initial peak crushing force are similar for both cases, although the initial stiffness of multi-layer TSP foldcore is slightly lower than that of single-layer foldcore which is caused by the accumulated gaps between core and plates in each layer. The same base plate was used with a 2 mm boundary to constrain the in-plane movement during lateral crushing of the foldcore as shown in Figure 6. There was no bonding between the foldcore and the base plate. The loading speed was set as 1 mm/min and the specimens were crushed till around 80% of the total height. The design height of the foldcore is 20 mm for each layer and 3 mm for the base plate, slight gap between the base plate and the foldcore exists due to the imperfect preparation. This leads to a slightly higher overall height and a lower initial stiffness during crushing.

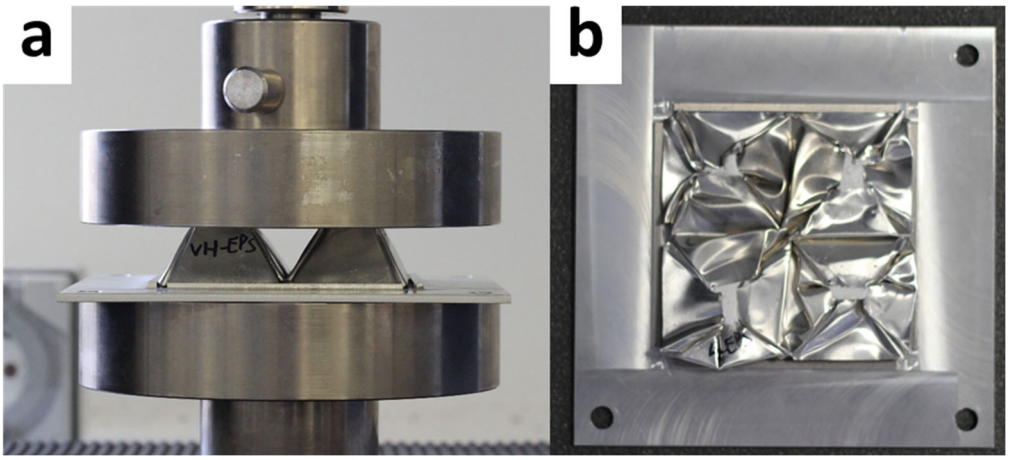

Figure 6. Single-layer cubic EPS28 foam filled TSP foldcore (a) during quasi-static crushing; (b) after crushing

177 The representative load-displacement curves of these foldcores under quasi-static crushing are
178 shown in *Figure 7*. Uniform and smooth crushing responses are demonstrated for all foam
179 configurations. Conventional cellular structures such as Miura-type foldcore [1], honeycomb
180 [28] and lattice structure [29] often have non-uniform crushing responses under quasi-static
181 and dynamic crushing, where a relatively large initial peak stress is followed by a sudden
182 decrease in crushing resistance and fluctuation of crushing load throughout deformation. As
183 shown, single-layer foam filled TSP foldcore has no obvious initial peak and the crushing
184 resistance is rather uniform throughout the deformation till crushed distance reaching
185 densification stage at around 60% to 70% of the overall height. This crushing behaviour is very
186 similar to foam materials and is ideal to be used as core sandwich structure for energy
187 absorption purposes [19]. With foam filler, the crushing resistance increases without inducing
188 an initial peak force. For the EPS foam filled foldcore, the heavier foam yields a higher
189 enhancement in crushing resistance of foldcores and this enhancement is much greater than the
190 crushing resistance of the foam itself. For instance, the average crushing resistance of foam
191 fillers alone is estimated ranging between 180 N and 410 N, from the measured foam
192 compressive strength and the cross-section area of foam fillers as shown in Figure 3 (a, b). As
193 given in Table 3, the average crushing resistance of TSP foldcore increases from 1.43 kN to
194 2.55 kN by adding the foam filler. This increase of 1120 N is much higher than the average
195 crushing resistance of foam fillers alone, indicating the interaction between TSP foldcore and
196 the infilled foam further enhances the impact resistance. Similar foam-wall interactions have
197 been investigated and sometimes the contribution from the interaction is greater than the
198 compressive strength of the added foam itself [23]. This also explains the significant increase
199 in crushing resistance of PU shaped foam filled foldcore. This is because that the shaped foam
200 has the similar geometry as the TSP foldcore as shown in Figure 2. The shaped foam provides

higher constraint to the entire sidewalls throughout crushing than cubic foam filler which has gaps between sidewalls and foam surfaces.

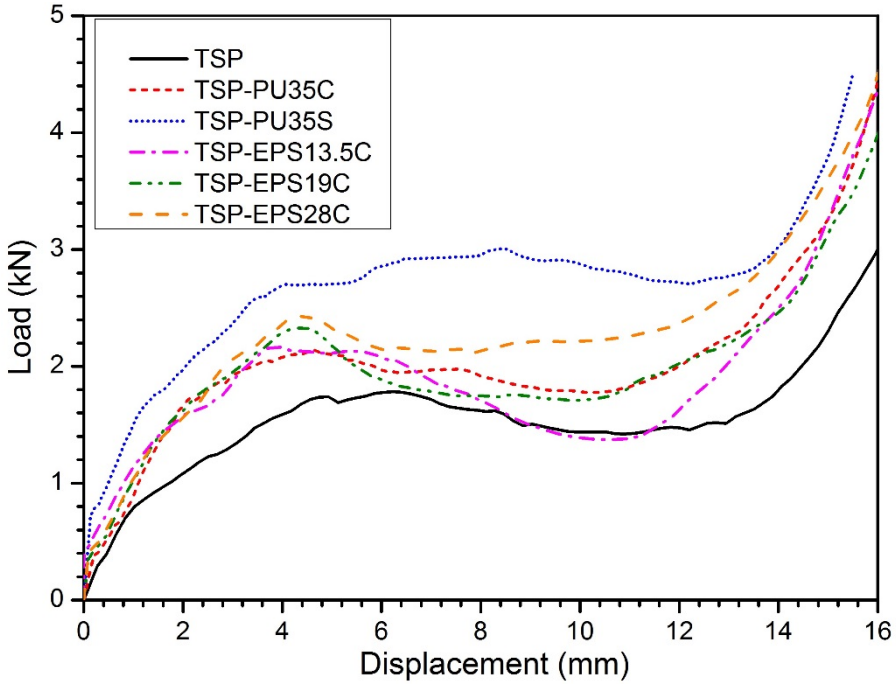

Figure 7. Representative load-displacement curves of TSP foldcore with different foam filler configurations under quasi-static crushing

The results including peak and average crushing force, P_{peak} , P_{ave} , increment in P_{ave} , uniformity ratio, U, densification strain ε_D , and specific energy absorption, SEA are listed in Table 3. In this study, the peak force is taken as the peak value before crushed distance reaches 50% of total core height, this is because that crushing force near densification for some cases could be higher due to the very uniform crushing response of the foldcores. As for many cellular structures, the peak force often occurs at the initial stage of the crushing. Densification crushed distance is defined by the sudden increase of crushing force at the later stage due to compaction of material and is estimated by the starting point of a consistent high slope over a certain distance in the load-displacement curve. Other parameters are calculated as follows

$$P_{ave} = \frac{\int_0^{h_D} P(\mathrm{h}) \cdot dh}{h_D} \tag{1}$$

$$SEA = \frac{\int_0^{h_D} P(\mathrm{h}) \cdot dh}{m_{TSP} + m_{foam}} \tag{2}$$

$$\varepsilon_D = \frac{h_D}{H} \tag{3}$$

where P is the crushing force, h is the crushed distance, h_D is the crushed distance at densification, m_{TSP} and m_{foam} are the mass of TSP foldcore and foam filler, respectively, ε_D is the densification strain, H is the overall height of the foldcore.

Foam filler configurations	P_{peak} (kN)	P_{ave} (kN)	Increment in P_{ave}	U= P_{peak} /P_{ave}	ε_D	SEA (J/g)
TSP	1.78	1.43	-	1.245	0.70	2.16
TSP-EPS13.5C	2.17	1.65	15.4%	1.312	0.61	2.11
TSP-EPS19C	2.33	1.82	28.0%	1.280	0.71	2.64
TSP-EPS28C	2.43	2.06	44.1%	1.180	0.68	2.79
TSP-PU35C	2.14	1.81	26.6%	1.182	0.68	2.40
TSP-PU35S	3.01	2.55	78.3%	1.180	0.69	3.14

Table 3. Summary of crushing response of single-layer foam filled foldcores under quasi-static crushing

The increase in average crushing force of foam filled TSP foldcore is obvious. Up to 78.3% increase is observed for PU shaped foam filled foldcore than TSP foldcore without foam while the uniformity ratio remains similar. This is due to the inclined geometry of TSP foldcore sidewalls which are connected via triangular interconnections. This unique geometry reduces the initial stiffness of the structure as compared to straight tubes, honeycombs and Miura-type foldcores. The interaction effect between foam and foldcore walls remains, resulting in a higher average crushing force. Likewise, the specific energy absorption of the foam filled foldcore is higher than that of TSP without foam filler, except TSP-EPS13.5C which has a lower

densification strain. A 45% increase in SEA is shown for shaped PU foam filled foldcore, from 2.16 to 3.14 J/g while the mass and density increment is 20.4% over the case without foam filler. For comparison, these foam filled foldcores have much higher SEA than many conventional energy absorbing aluminium structures with similar relative densities (2.7% for TSP foldcore without foam filler), e.g. SEA of CYMAT aluminium foam ranges between 0.5-0.8 J/g (3.1% relative density), aluminium eggbox with constrained boundary is around 1 J/g (2.8% relative density) and aluminium eggbox (3.5% relative density) with bonded boundary is about 2 J/g [30]. Al 1050 H111 alloy was used for the eggbox preparation in the above-mentioned study, which has similar mechanical properties and chemical composition (minimum 99% aluminium by weight [31]) as Al 1060 alloy used in this study.

3.2 Dynamic crushing test

High speed testing machine INSTRON VHS 160/100-20 is used for dynamic crushing tests of foam filled multi-layer TSP foldcore, as shown in Figure 8. Both crushing head and base support are cylinders with the diameter of 100 mm. High speed camera Fastcam APX RS is used to capture the deformation process. Frame rate is set to 5,000 fps for this study. The setup shown in Figure 2 (c) is used for the dynamic crushing tests. Neither glue nor bonding is used between these layers. Only one set of plates and rods are used for all of the tests. Overall design height is 69 mm including three layers of 20 mm high TSP foldcore with different foam filler configurations and three 3 mm-thick plates, each with a 2 mm boundary to constrain the in-plane movement of foldcore sidewalls. The actual overall heights, however, are around 71-74 mm due to the manual folding induced gaps between foldcores and plates. Core densities of foam filled three-layered TSP foldcore are listed in Table 4, which are calculated using the volume of 80x80x20 mm, similar to the volume used in the relative density calculation of TSP foldcore without foam infill. Three specimens are tested for each configuration, and the representative curve from three test results is selected for result analysis.

Foldcores	3TSP	3TSP-EPS13.5C	3TSP-EPS19C	3TSP-EPS28C	3TSP-PU35C	3TSP-PU35S
Core density (kg/m^3)	73	75	77	78	80	88

Table 4. Core densities of three-layered foam filled TSP foldcores for dynamic crushing test

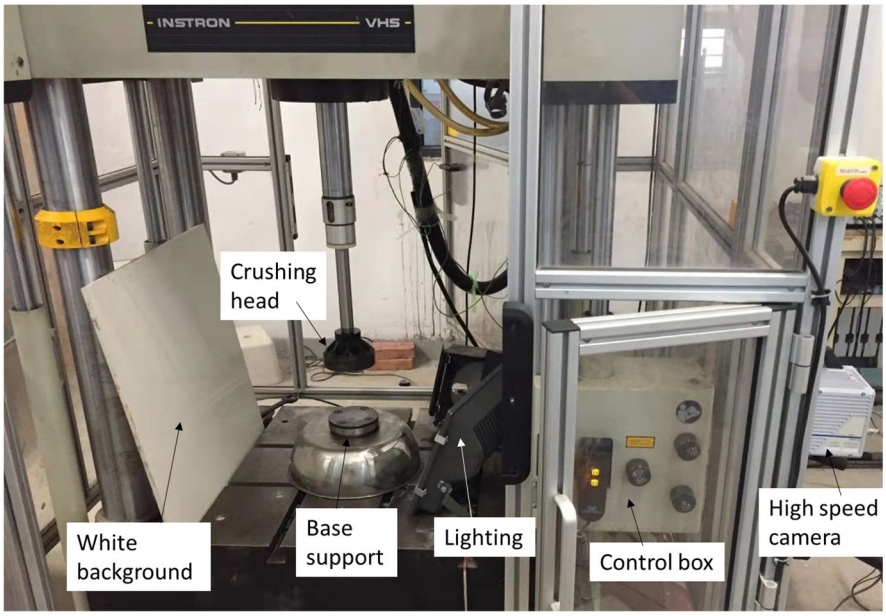

Figure 8. High speed testing machine INSTRON VHS 160/100-20

3.2.1 Dynamic crushing speed

The crushing speed was set as 10 m/s for all tests. This machine uses servo-hydraulic and control technologies to provide a constant crushing speed. However, due to the limitation of sample height, the actual crushing speed is not constant throughout the crushing process especially towards the later stage of crushing. The loading process of the crush head includes three parts: accelerating from zero speed at some distance above sample, then travelling at nearly constant speed followed by decelerating to zero speed before reaching the end position. As the overall height of the 3-layered TSP foldcore is about 71 mm, the crush head is at the decelerating stage when it is in contact with the testing sample. As shown in Figure 9 (a), the gradient of the time-displacement curve decreases over time and becomes almost flat at around 45 mm of crushed distance, indicating a decreasing crushing speed over the deformation of the

sample. It is also worth noting that the actual impact speed is slightly smaller than the desired moving speed of 10 m/s when the crushing head is in contact with the sample. As the actual crushing speed is not a constant value, the crushing speed in this study only refers to the designated speed of the test, instead of the actual crushing speed. The maximum strain rate demonstrated in this study is calculated around $150s^{-1}$, which is a typical intermedia strain rate [32].

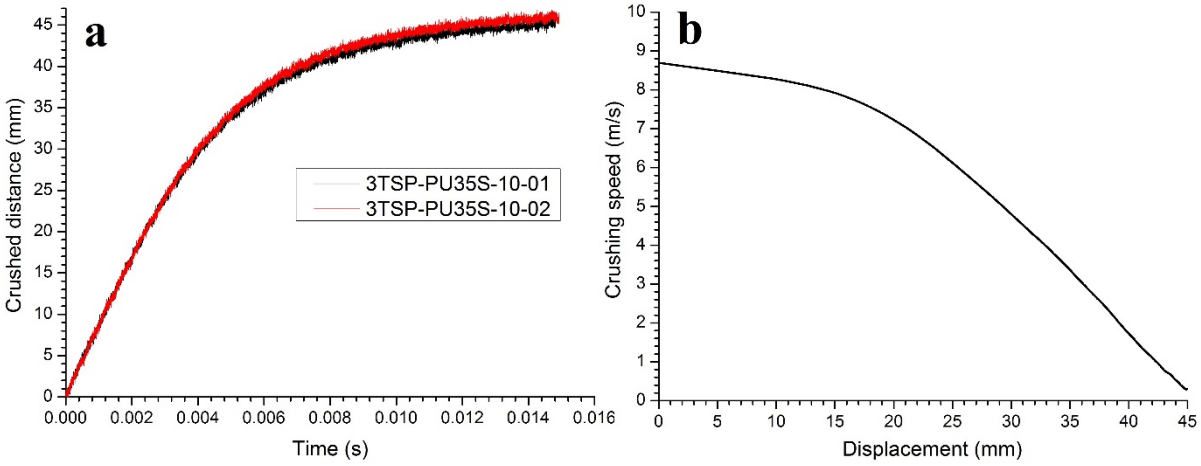

Figure 9. (a) Unfiltered displacement time histories of crush head under 10m/s crushing; (b) smoothed actual displacement-crushing speed curve under 10 m/s crushing

3.2.2 Results comparison

The load-displacement curves of multi-layer foldcore samples under 10 m/s dynamic crushing are shown in *Figure 10*. The results of these six different foam filler configurations are shown separately in two charts for clarity. Fluctuations are shown in all the curves under dynamic crushing as compared to quasi-static loading conditions in the previous section. Distinct enhancements in crushing resistance are observed for TSP foldcore with foam filler. As expected, heavier foam provides higher enhancement of crushing resistance to the multi-layer foldcore, as higher density leads to higher plateau stress for the same type of foam material. Furthermore, the structure with shaped PU foam filler has a much higher crushing resistance

than the structure with cubic PU foam filler, as shaped foam has a larger mass than cubic foam and better support is provided by the shaped foam to the inclined sidewall of TSP foldcores. It is also noted that the initial stiffness of the structures is relatively low at the very beginning of the deformation around 0-3 mm displacement. This is caused by the incomplete contact of the foldcores and plates as mentioned in the previous section. Due to the fabrication induced imperfections, slight gaps exist between foldcore and plate at each layer, which lowers the initial stiffness at the early stage of the loading.

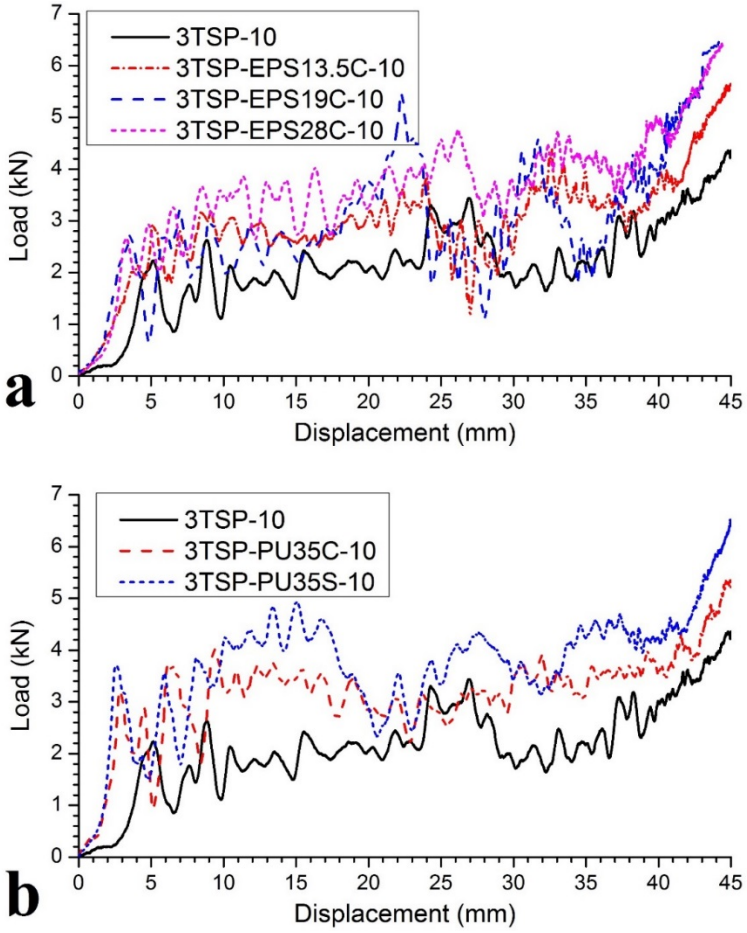

Figure 10. Load-displacement curves of (a) EPS foam filled multi-layer TSP foldcores; (b) PU foam filled multi-layer TSP foldcores; under 10 m/s crushing

Other data of structural response are listed in Table 5. Similar to the previous section, the densification strain, ε_D is estimated by the crushed distance where the sudden increase of

297 crushing force occurs, dividing the overall height of the foldcore. The average crushing force
298 is averaged from the beginning till the densification of the core. The densification strains of
299 these foam filled foldcore under 10 m/s crushing are similar to single-layer foldcores crushed
300 under quasi-static loading condition. The uniformity ratio, which is the ratio between peak and
301 average crushing force, remains between the values of 1.32 to 2.05, which is slightly higher
302 than the quasi-static crushing of the single-layer foldcore. This increase is caused by the
303 dynamic effect of the foldcore structures and the interaction with the foam material. This may
304 be also caused by the fluctuation in recording data under 10 m/s loading rate. However, this
305 slight increase in uniformity ratio with increasing crushing speed is minimal comparing to
306 many conventional structures, such as honeycomb, cube strip and Miura-type foldcore, where
307 their peak crushing force as well as uniformity ratio can increase several times under dynamic
308 loading [1, 3, 15, 33] as compared to the quasi-static loading condition.

Foam filler configurations	**P_{peak} (kN)**	**P_{ave} (kN)**	**Increment in P_{ave}**	**$U= P_{peak} / P_{ave}$**	**ε_D**	**SEA (J/g)**
3TSP-10	3.44	1.94	-	1.773	0.65	2.70
3TSP-EPS13.5C-10	4.38	2.69	38.7%	1.628	0.63	3.53
3TSP-EPS19C-10	5.44	2.65	36.6%	2.053	0.59	3.20
3TSP-EPS28C-10	4.76	3.40	75.3%	1.400	0.68	4.62
3TSP-PU35C-10	4.01	3.04	56.7%	1.319	0.71	4.25
3TSP-PU35S-10	4.92	3.53	82.0%	1.394	0.70	4.41

309 Table 5. Summary of crushing response of multi-layer foam filled foldcores under 10m/s
310 crushing

311 Significant improvement in both the average crushing force and specific energy absorption can
312 be observed for all foam filled structures. The increases in average crushing force and specific
313 energy absorption for foam filled structure are ranged from 36.6% to 82% and from 18.5% to
314 71.1%, respectively. Among these five foam filler configurations, shaped PU foam filled TSP
315 foldcore has the highest average crushing resistance, i.e., 82% higher than that without foam

316 filler. As explained in the previous sections, due to the matching geometry of the shaped foam
317 to the inclined sidewalls of foldcore, the shaped foam provides better support to the sidewalls
318 than cubic foam under lateral crushing. EPS28 cubic foam filled TSP foldcore, however, has
319 the highest specific energy absorption among these foam configurations. As shown in *Figure*
320 *5*, the EPS28 foam material has higher crushing resistance than PU35 material especially at the
321 later stage of the crushing.

3.3 Damage modes

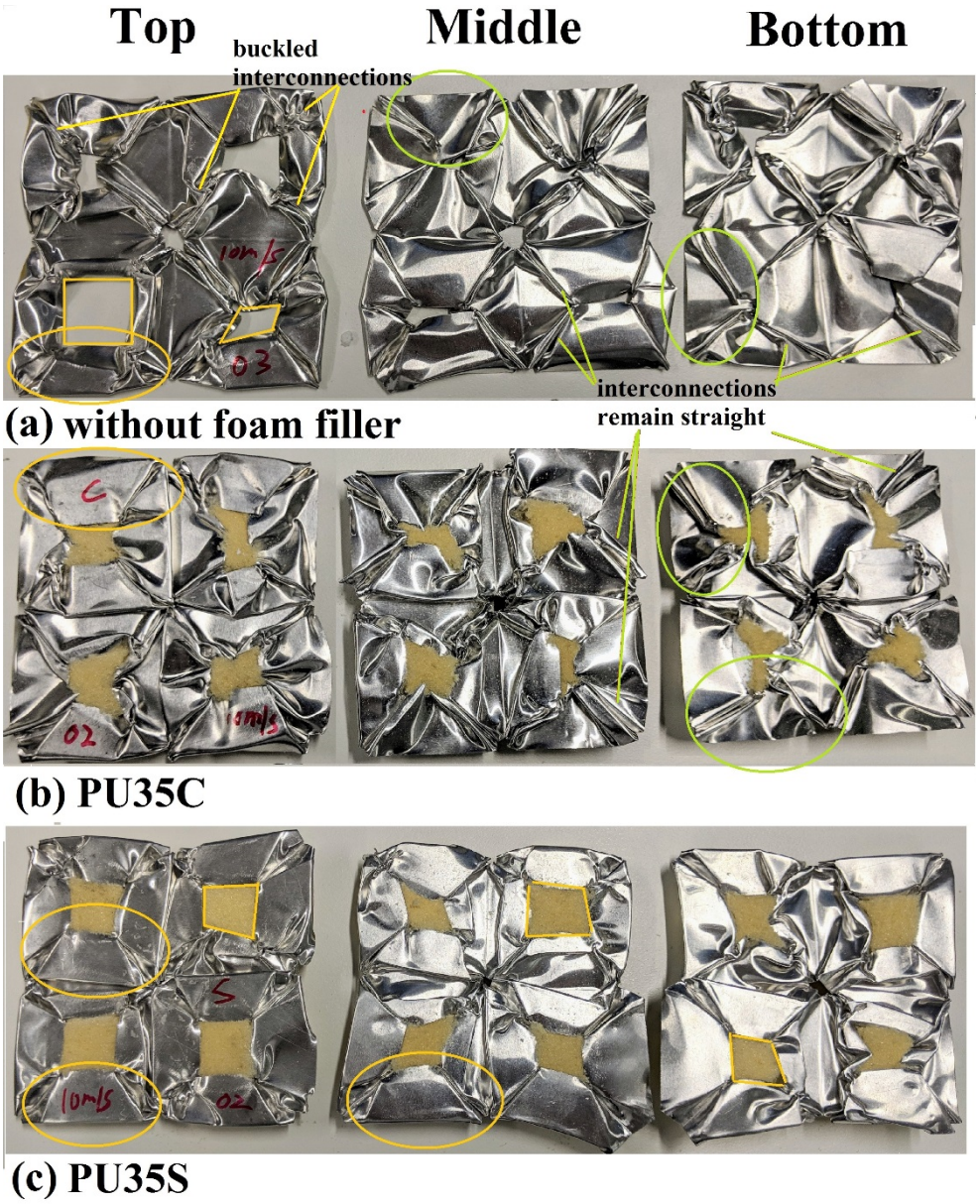

Figure 11. Damage modes of individual layers of (a) TSP foldcore without foam, (b) with cubic PU foam and (c) with shaped PU foam after crushing, two damage modes are marked out in yellow and green

Damage modes of these foam filled multi-layer foldcores are shown in Figure 11 and Figure 12. For TSP foldcore without foam filler, two distinct damage modes are observed on different layers. On the top layer, the sidewalls bend towards outside horizontally, the top edges around

330 the square opening remains its shape as marked out in yellow colour in Figure 11. The
331 interconnections which connect the adjacent sidewalls are buckled and twisted on the top layer.
332 No corner lift-up is observed for this damage mode on the top layer. For the middle and bottom
333 layers of TSP foldcore without foam filler, the damage mode of the structure is quite different.
334 Sidewalls bend inwards along their vertical middle line of the trapezoid sidewalls as circled in
335 green colour. This results in the deforming of the top edge sidewalls, therefore the square
336 shaped openings of the middle and bottom layers are no longer square after crush test. The
337 interconnections are less deformed in this damage mode and remain straight as marked out in
338 the figure. Furthermore, corner lift-up can be observed as well in this damage mode. A
339 computed damage modes comparison between the top and middle layer of TSP foldcore
340 without foam filler is shown in Figure 16 for illustrating the difference of these two damage
341 modes. This change in damage mode is caused by the increase of loading rate and the inertia
342 effect of the top layer under dynamic impact of the crush head. As previously studied [15], the
343 damage mode of TSP foldcore changes from the vertical inward bending of sidewalls (marked
344 in green) to outwards horizontal bending (marked in yellow) with the increasing loading rate.
345 For these tests, the crushing speed is different at each layer. The top layer experiences the
346 highest crushing force once the crushing head and foldcore are in contact and the crushing
347 speed is continuously reduced to zero once it reaches 45 mm of stroke as shown in Figure 9
348 (b).

349 For the cubic PU foam filled TSP foldcore under dynamic crushing, the corresponding damage
350 mode of each layer is similar to those without infilled foam. The square openings remain their
351 shapes after crushing and sidewalls bend towards outside with almost no corner lift-up
352 observed on the top layer. Other damage mode is observed on the middle and bottom layers.
353 The square openings of the middle and bottom layers are not fully closed in this case as
354 compared to TSP foldcore without foam infill. This is due to the extra resistance at each unit

cell centre provided by the added foam material. The shaped PU foam filled TSP folded structure has a quite different damage mode as comparing with the cases of no foam filler and with cubic PU foam filler. Only one damage mode is presented on all three layers for the shaped PU foam filled structure. No inward vertical bending of the sidewalls occurs on the middle and bottom layers which are presented in both the previous two cases (no foam filler and cubic PU foam filler). The corner lift-up does not occur for all three layers either. Due to the presence of shaped PU foam, the damage mode associated with sidewalls inwards vertical bending is much harder to occur. Shaped foam provides much more support to the sidewalls as they both have similar geometries. Therefore, it is easier for sidewalls of foldcore to bend outwards horizontally as in the first damage mode. It is also worth noting that some part of foldcore expends outside the boundary after crushing as shown in Figure 11 (c). This might be caused by the compression of the shaped foam around the outer edges.

As shown in Figure 12, EPS foam filled multi-layer TSP foldcore shows similar damage modes with the corresponding layers of TSP foldcore and cubic PU foam filled foldcore. Both damage modes are presented in all three cubic EPS foam configurations. The square openings at the centre of each unit cell better remain their square shapes with the heavier foam filler added, as can be seen from EPS13.5C to EPS19C to EPS28C. The heavier foam filler has a higher compressive strength which provides more support to the top edges of the sidewalls. Therefore, with the heavier foam, it is harder for foldcore sidewalls to undergo vertical inwards bending and the top square opening can better remain their shape.

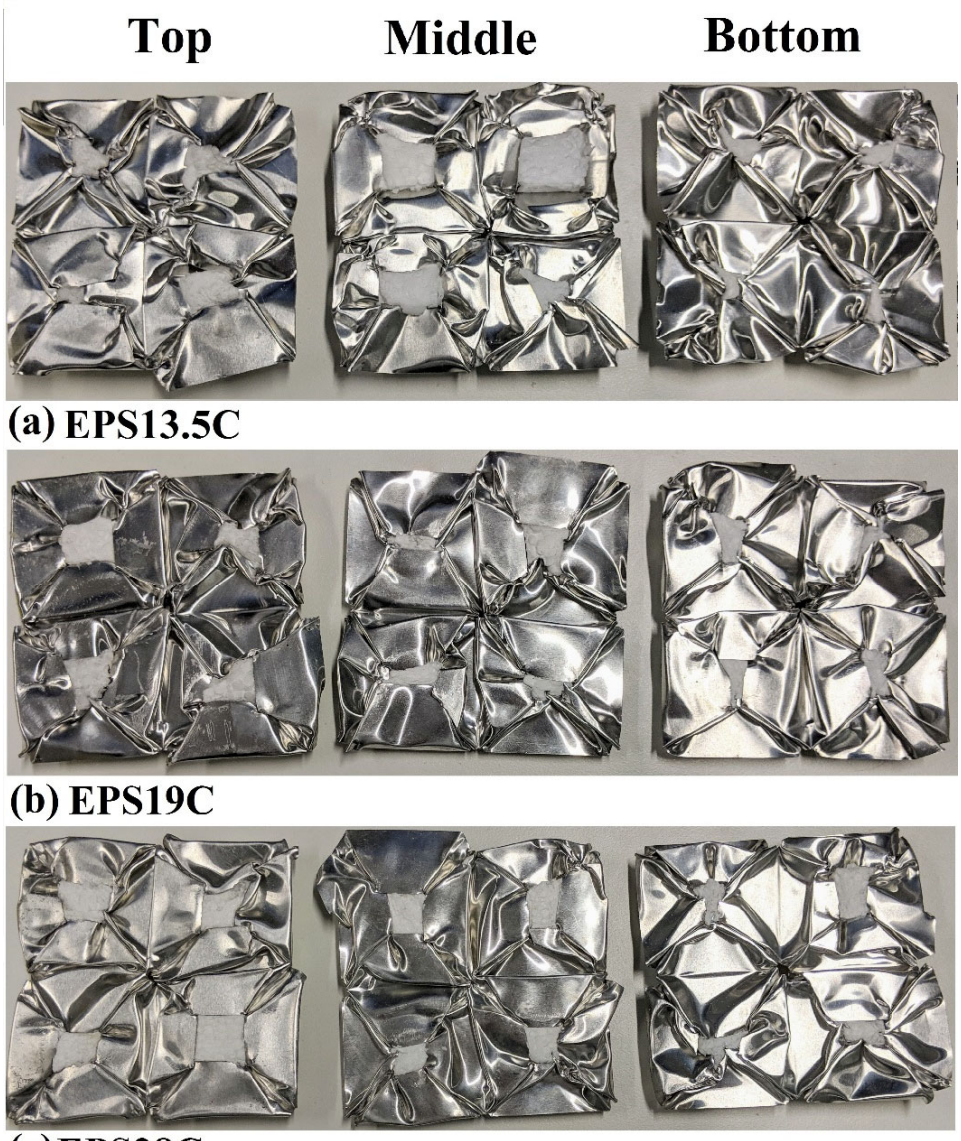

375

376 Figure 12. Damage modes of individual layers of different EPS cubic foam filled foldcores

377 under crushing

4. Finite element analysis

4.1 Finite element model

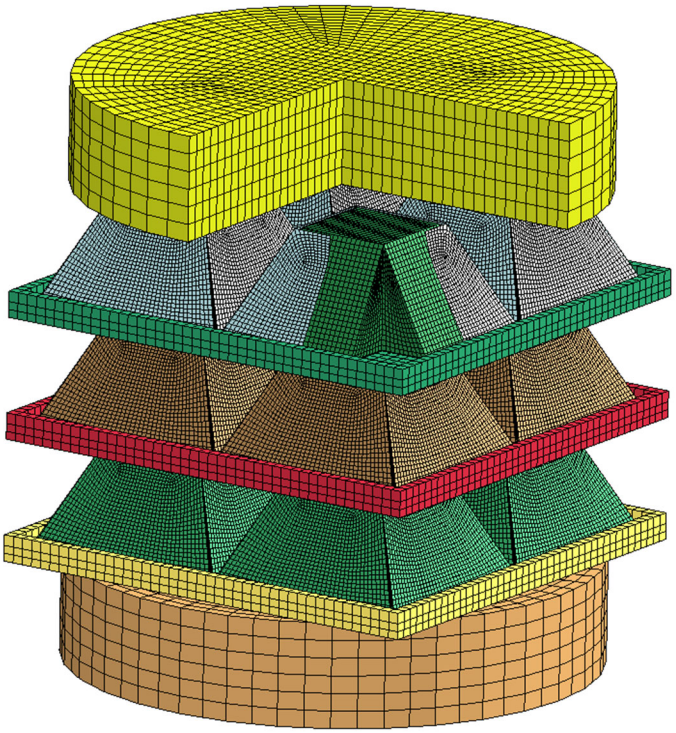

Figure 13. Numerical model of crushing setup for shaped foam filled three-layered TSP foldcore; note: portion of crushing disk and top layer TSP foldcore is removed for illustration

Finite element analysis of these foam filled multi-layer TSP foldcores was carried out. Finite element software LS-DYNA is used for the simulations. The TSP foldcores were modeled using shell element and the foam material, plates and crushing disk are modelled using solid element. 2 mm high boundary of the plates were modelled as well as shown in Figure 13. The cylindrical crushing disk and base have the diameter of 100 mm. As observed in the crushing test, the deformation of the interlayer plates between foldcore layers was minimal and therefore ignored in the numerical simulation. Interlayer plates, base support and top crushing disk were all modelled as rigid block. Base support was fixed in all six degrees of freedom and crushing

391 disk is fixed in five degrees of freedom with lateral movement allowed. No constraint was
392 applied on the interlayer plates.

393 To minimize the uncertainties, the actual crushing speed of the crushing disk derived from the
394 dynamic crushing test shown in Figure 9 (b) was applied on the crushing disk in the numerical
395 models to simulate the changing crushing speed. Material parameters used for EPS, PU foam,
396 1060 aluminium sheet and aluminium 5083 alloy are listed in section 2. Neither glue nor other
397 fixing was considered in the numerical models, same as in the experiment. A friction
398 coefficient of 0.25 was considered for all interfaces. Mesh convergence tests of both TSP
399 foldcore and foam material have been carried out in the previous study [14].

400 ### 4.2 Comparison with experimental results

401 The load-displacement curves of these multi-layer TSP foldcores with different foam filler
402 configurations under 10 m/s crushing are shown in Figure 14. The average crushing forces and
403 peak crushing forces from both the FE simulation and tests are marked out for all the cases.
404 Overall, the FE results match well with the test data. The initial peak force at around 5 to 10
405 mm displacement match well between the two curves for all cases. This first initial peak force
406 corresponds to the initiation of the sidewall buckling of the TSP foldcore. The average crushing
407 forces are in good agreement as well, while some large fluctuations in the later stage are
408 observed in the numerical results. Displacement fluctuations of 3TSP-10 (20-30mm), 3TSP-
409 EPS19C-10 (28-35 mm) and 3TSP-PU35S-10 (27-37 mm) are captured in numerical
410 simulations and well match the experimental data. These fluctuations correspond to some
411 collapsing of the layers. However, the initial stiffness of the structures in all cases from finite
412 element results is higher than the test data. The gradient of all FE curves at initial stage (0 to 2
413 mm displacement) is higher than the test data. As mentioned in the previous section, this is due
414 to the imperfections induced during the sample preparation. Minor bending of the sidewalls,

415 slight gaps between foldcore and plates can lead to the lower initial stiffness. The focus of this
416 study is to observe the crushing behaviour and examine the energy absorption of the proposed
417 foam filled folded structures, therefore these minor discrepancies between the FE and test
418 results can be neglected. The overall crushing behaviour and energy absorption from both the
419 numerical simulations and tests match well under the large deformation of the structures.

420 Parameters including peak and average crushing force, densification strain and specific energy
421 absorption from both FE and experimental data of these foldcores are listed in Table 6. Similar
422 to the load-displacement curves, the average crushing forces are in good agreement for the
423 foam filled foldcores, while discrepancies exist between FE and test results for TSP foldcore
424 without foam filler. Relatively smaller discrepancies of the cases with foam filler indicate that
425 the added foam may help mitigate some of the effect caused by imperfection during specimen
426 preparation. For the case without foam filler, imperfections on sidewalls may locally change
427 the deformation mode of foldcore. With cubic or shaped foam material added in the centre of
428 each unit cell of the foldcore, extra support provided to foldcore sidewalls makes vertical
429 inwards bending more difficult to initiate and reduces the influence of local imperfections.
430 Higher density of foam filler tends to increase the crushing resistance and the specific energy
431 absorption of the structure. Structure with shaped PU35 foam has the highest average crushing
432 resistance, while cubic EPS28 foam filled structure possess the highest SEA due to the stronger
433 yet lighter EPS foam material.

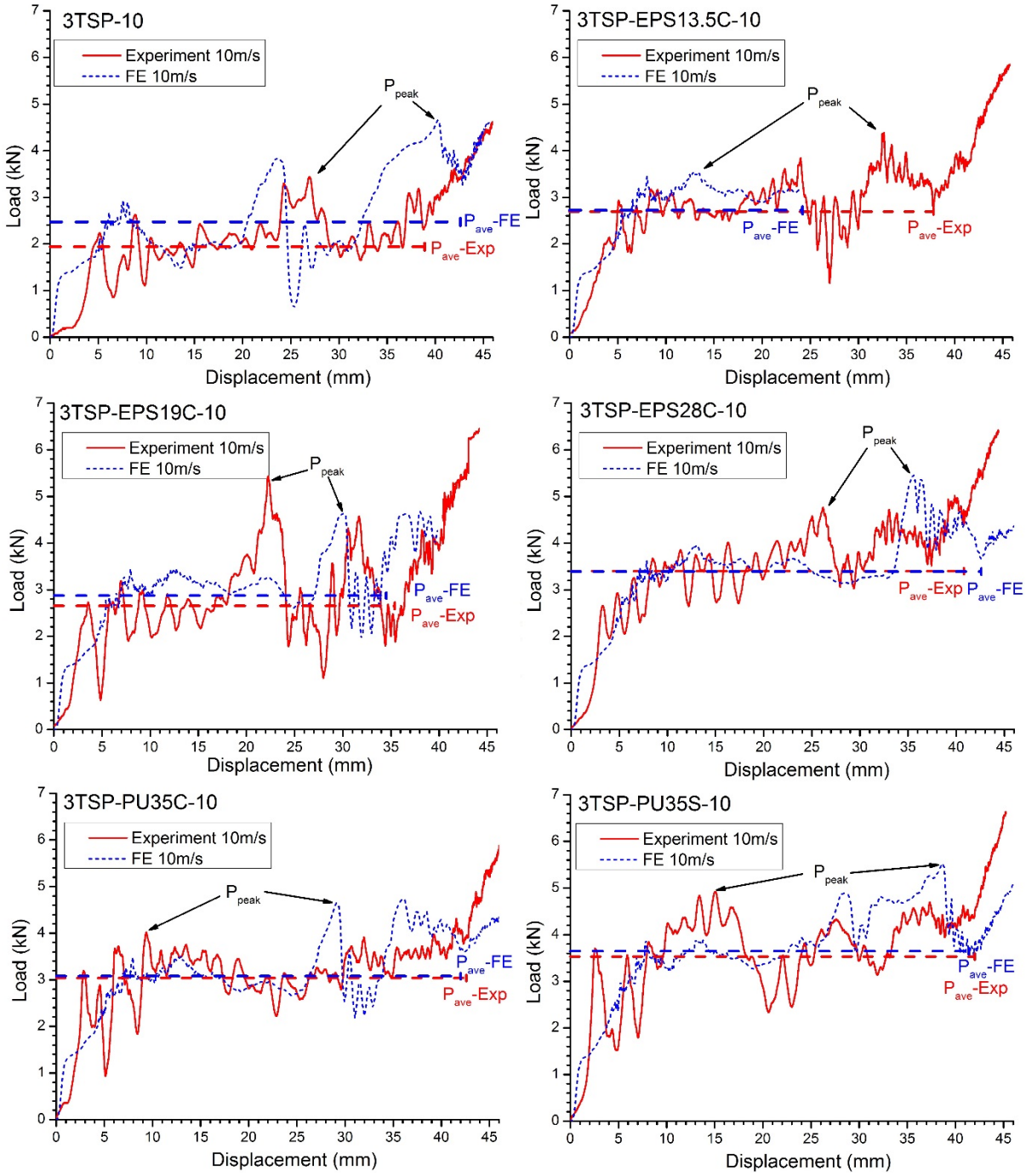

Figure 14. Load-displacement curves of multi-layer TSP foldcores with five foam configurations under 10 m/s crushing

Foam filler configurations	P_{peak} (kN)		P_{ave} (kN)		ε_D		SEA (J/g)	
	Exp	FE	Exp	FE	Exp	FE	Exp	FE
3TSP-10	3.44	4.65	1.94	2.47	0.65	0.71	2.70	3.79
3TSP-EPS13.5C-10	4.38	-	2.69	2.72	0.63	-	3.53	-

3TSP-EPS19C-10	5.44	4.65	2.65	2.87	0.59	0.58	3.20	3.38
3TSP-EPS28C-10	4.76	5.46	3.40	3.39	0.68	0.71	4.62	4.71
3TSP-PU35C-10	4.01	4.64	3.04	3.08	0.71	0.70	4.25	4.24
3TSP-PU35S-10	4.92	5.52	3.53	3.65	0.70	0.69	4.41	4.52

438 Table 6. Comparisons between FE and experimental data of multi-layer foldcores with different
439 foam filler configurations Note: Due to large deformation of the foam material and the
440 significant difference of elastic modulus between aluminium 1060 sheet and EPS13.5, the
441 numerical simulation of 3TSP-EPS13.5C-10 terminates half way and the numerical results are
442 not presented herein.

443 ### 4.3 Comparison of damage modes

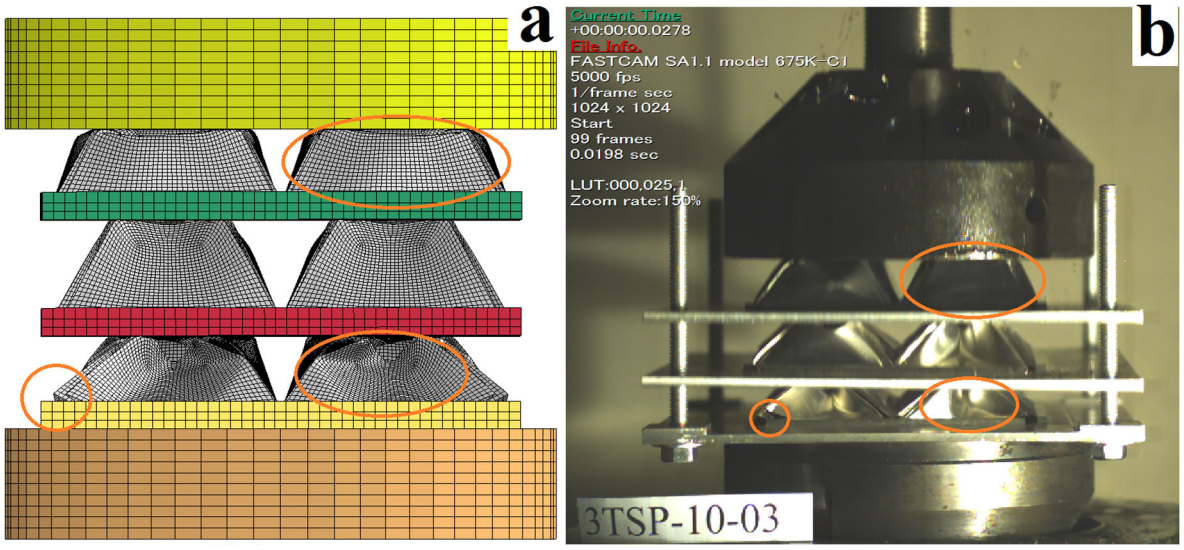

444

445 Figure 15. Damage modes of TSP foldcore without foam fillers in (a) FE simulation and (b)
446 crushing test at around 15 mm displacement

447 The comparison of multi-layer TSP foldcore without foam filler at around 15 mm of crushed
448 distance is shown in Figure 15. The damage mode from numerical simulation agrees well with
449 that observed in the test. Comparison of the damage modes on the top and middle layers of
450 TSP foldcore without foam filler obtained from numerical simulation is shown in Figure 16.
451 For the top layer of this multi-layer foldcore, the sidewall bends out horizontally near the

middle of this layer. For the middle and bottom layers, however, the sidewalls bend vertically towards centre of the unit cell. This damage mode leads to lift-up of the corners and the joint lines connecting the adjacent sidewalls remain straight in the middle and bottom layers. As shown in Figure 11 (a), the interconnections are buckled and twisted under the first damage mode of the top layer.

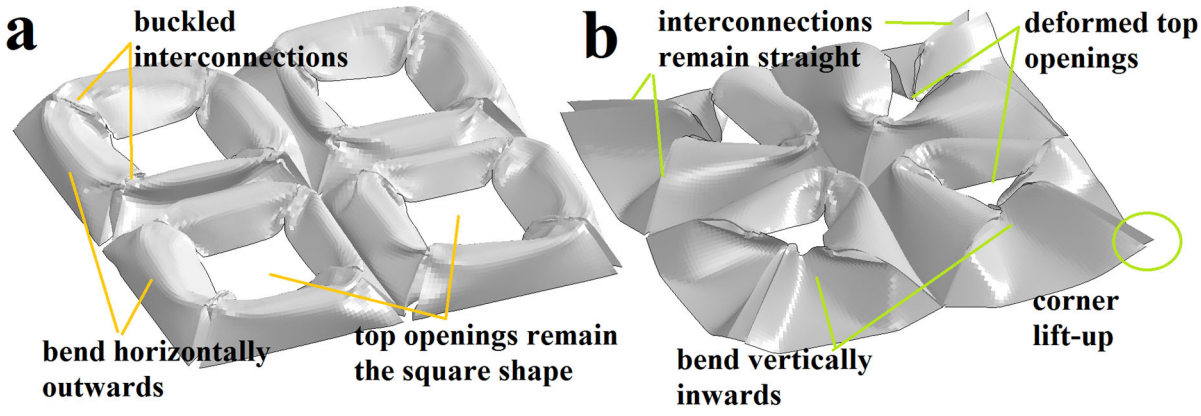

Figure 16. Computed damage modes of TSP foldcore without foam filler under 10m/s crushing on (a) top layer; (b) middle layer, note: these images are not captured at the same time

The computed damage modes of three typical foam filled multi-layer TSP folded structures are shown in Figure 17. Three sets of damage modes are presented on these three structures and the similarity in damage mode of each set is demonstrated with crushing tests. For TSP folded structure without foam filler, the top layer shows different damage mode from the middle and bottom layers. The sidewalls bend horizontally outwards, resulting in the top square opening of each unit cell remains their shape and no corner lift-up is observed. As for the middle and bottom layers, the outer sidewalls bend vertically towards the centre of each unit cell, therefore resulting in the deformation of the top square opening and leading to corner lift-up, which can be also observed on the bottom layer shown in Figure 15. For the folded structure with cubic EPS28 foam filler, the damage modes are similar to the case without foam filler. The square

471 openings are clearly demonstrated on the top layer, while these are more or less deformed on
472 the middle and bottom layers. Due to the resistance provided by the filled cubic foam, these
473 openings are less deformed after crush, while the openings are almost fully closed due to the
474 deformation for the case without foam filler. Less corner lift-up on the middle and bottom
475 layers of the EPS foam filled structure is displayed for the same reason. Only one type of
476 damage mode is shown in three layers of shaped PU foam filled TSP folded structure. Only
477 horizontal bending and buckling of the sidewalls are presented, therefore the top edges of the
478 sidewalls remain straight and the square openings are not deformed after crush. The shaped
479 foam has the almost identical slope as the inclined walls of the TSP folded structure, which
480 provides resistance and interacts with the cell walls during the deformation. This leads to the
481 change of damage mode for the middle and bottom layers and the improvement in crushing
482 resistance under dynamic crushing as well.

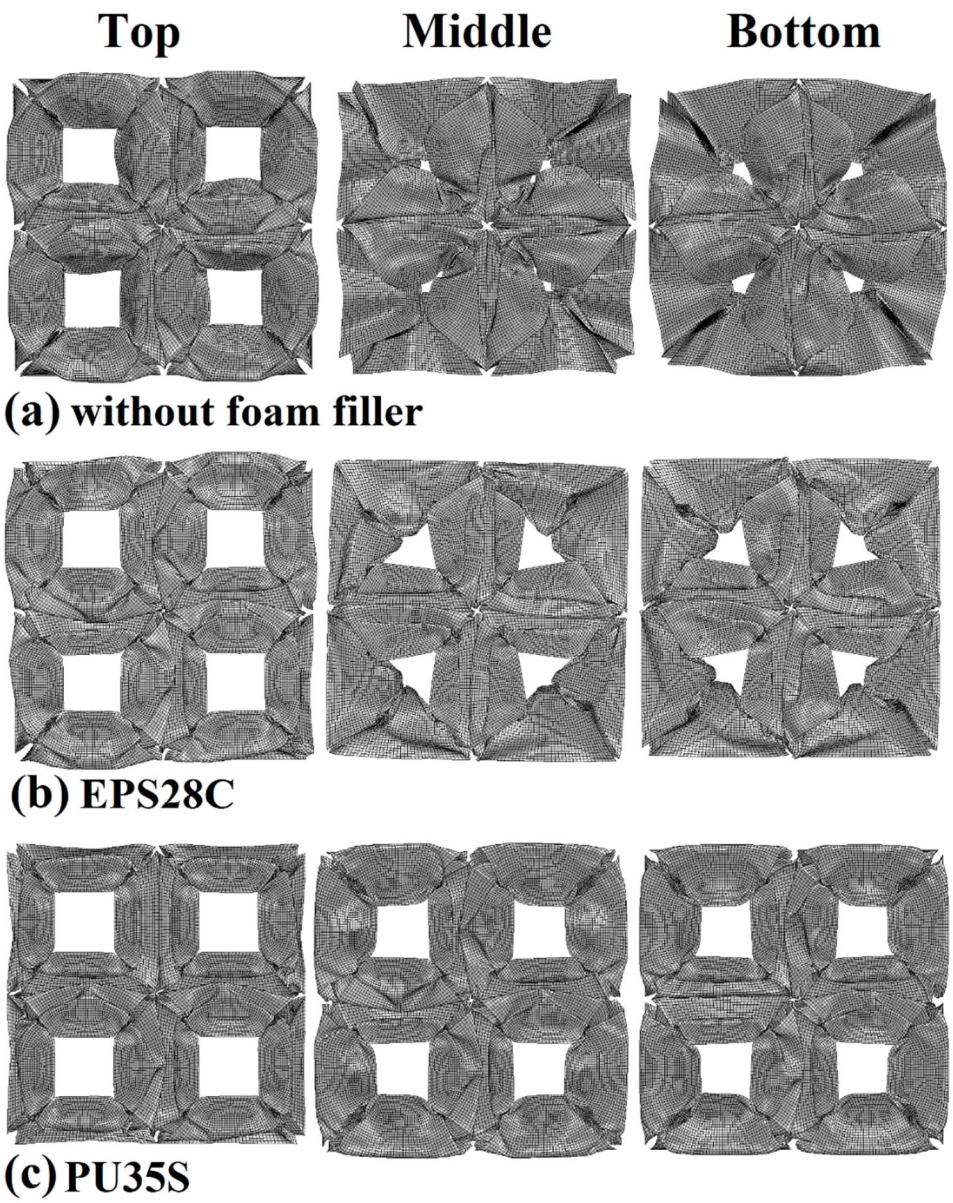

Figure 17. Damage modes of three layers of TSP foldcores without foam, with cubic EPS28 foam and with shaped PU35 foam after crushing

The correlated deformation modes of three layers of the shaped PU foam filled TSP folded structure are shown in Figure 18. The side views of the folded structure from both high speed camera images and FE simulation are compared. For load-displacement curve of test result, three peak value can be identified, and these three peaks correlates to the buckling of the middle, bottom and top layer, respectively. Slight tilting of the interlayer plates and uneven deformation of same-layer unit cells are also observed, this resulting the slight fluctuation of the load-

displacement curve as compared to FE results. For FE simulation of this foam infill configuration, the middle and bottom layer deform at same time, while bottom layer reached fully compacted state earlier than middle layer at about 27 mm of displacement. After the densification of bottom and middle layer, the half-crushed top layer start further buckling which results a peak in load at about 37 mm as marked. This layer crushing order is similar for both FE and test results, the corresponding crushed distance of the peak loads match quite well for both cases.

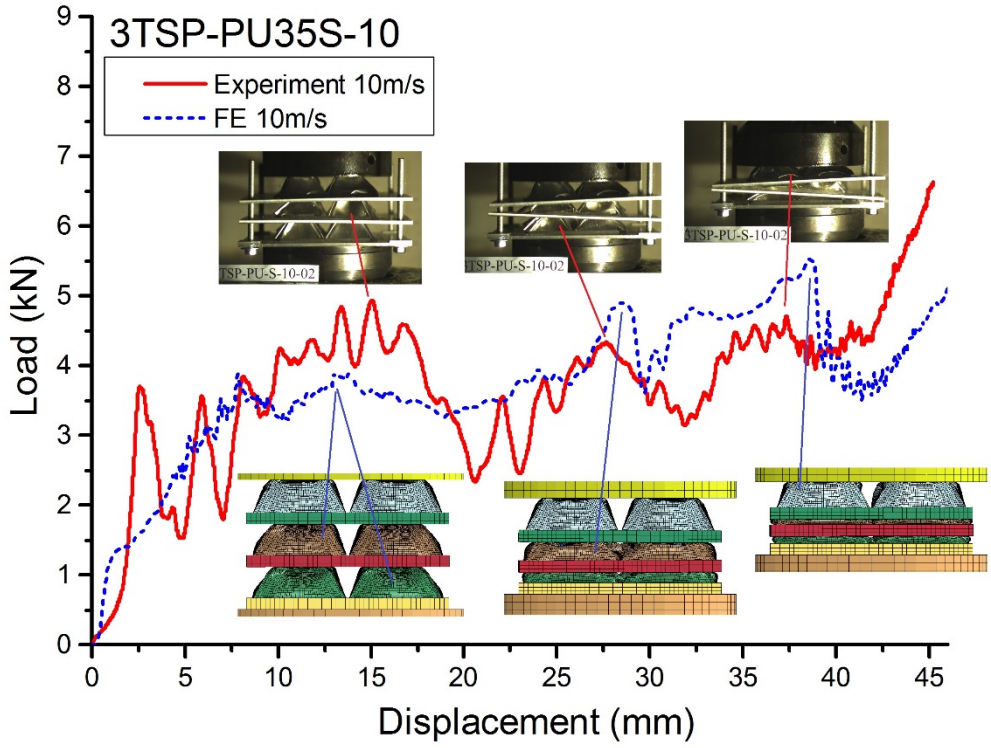

Figure 18. Correlation between layer deformation and load-displacement response of three layer shaped PU foam filled TSP folded structure under 10m/s crushing

Overall, the damage modes of both computed results and crush tests are in very good agreement. However, the deformation in FE results is more symmetric and uniform, whereas the deformation in crush tests is not necessarily symmetric and uniform. Furthermore, some bottom edges bend over the 2 mm high boundary of the inter-layer plates. All the foldcores stay well inside the boundary after the crushing. These discrepancies might be caused by the

imperfections of the samples and slight tilting of the interlayer plates during the crushing. As the slight gaps exist between foldcore and plates, sidewalls slightly bend during folding process and the unit cells of foldcore are not necessarily at the same height level. These leads to a slight reduction in initial stiffness of the structure, as well as the crushing resistance and energy absorption. More precise manufacturing process and better design of the multi-layer set-up could be applied in the future to minimize these imperfections.

5. Conclusions

Structural responses of foam filled multi-layer truncated square pyramid (TSP) kirigami structures under dynamic loading are investigated in experimental and FE analysis. Five different foam filler configurations are considered and compared to the case without foam filler. For these five cases: cubic EPS13.5, cubic EPS19, cubic EPS28, cubic PU35, shaped PU35 foam filler, the increase in crushing resistance and the improvement in specific energy absorption are demonstrated. Due to the interaction between the folded structure and the foam material, up to 82% increase in average crushing resistance is shown with only 3% to 20% increment in weight. Among these foam filler configurations, cubic EPS28 infill results in the highest increase in specific energy absorption (SEA), and shaped PU35 foam infill leads to the highest increase in average crushing force under dynamic loading, which is due to the higher compressive strength of EPS28 foam than PU35 foam. However, shaped foam shows a greater improvement in crushing resistance due to better interaction between foam and cell walls. The uniform crushing responses can be observed for all foam fillers with a uniformity ratio less than 2.0 under both quasi-static and 10 m/s crushing, whereas the uniformity ratio can reach 4.0 for some existing sandwich structures under dynamic crushing [15]. As discussed in section 3.1, the specific energy absorption of the proposed structure (2.16 to 3.14 J/g under quasi-static loading) is much higher than conventional cellular structure such as aluminium foam (0.5-0.8

J/g) and aluminium eggbox (1 to 2 J/g) of the similar density and similar material. This indicates great potential of the proposed foam filled multi-layer TSP kirigami structure for energy absorption applications. The verified numerical model can be used in further studies to predict the performances of the proposed sandwich structures with different parameters.

Acknowledgement

The authors acknowledge the support from Australian Research Council via Discovery Early Career Researcher Award (DE160101116). The authors acknowledge the assistance provided by Ms. Samantha Tyson from Curtin University for testing preparations.

References

[1] S. Heimbs, Foldcore sandwich structures and their impact behaviour: an overview, in: Dynamic failure of composite and sandwich structures, Springer, 2013, pp. 491-544.

[2] S. Heimbs, P. Middendorf, S. Kilchert, A.F. Johnson, M. Maier, Experimental and Numerical Analysis of Composite Folded Sandwich Core Structures Under Compression, Applied Composite Materials, 14, 2008, 363-377.

[3] A. Pydah, R.C. Batra, Crush dynamics and transient deformations of elastic-plastic Miura-ori core sandwich plates, Thin-Walled Structures, 115, 2017, 311-322.

[4] M. Schenk, S.D. Guest, G.J. McShane, Novel stacked folded cores for blast-resistant sandwich beams, International Journal of Solids and Structures, 51, 2014, 4196-4214.

[5] H. Fang, K.W. Wang, S. Li, Asymmetric energy barrier and mechanical diode effect from folding multi-stable stacked-origami, Extreme Mechanics Letters, 2017.

[6] J.M. Gattas, Z. You, Miura-Base Rigid Origami: Parametrizations of Curved-Crease Geometries, Journal of Mechanical Design, 136, 2014, 121404-121404-121410.

[7] J.M. Gattas, Z. You, The behaviour of curved-crease foldcores under low-velocity impact loads, International Journal of Solids and Structures, 53, 2015, 80-91.

[8] R.K. Fathers, J.M. Gattas, Z. You, Quasi-static crushing of eggbox, cube, and modified cube foldcore sandwich structures, International Journal of Mechanical Sciences, 101-102, 2015, 421-428.

[9] R. Xie, Y. Chen, J.M. Gattas, Parametrisation and application of cube and eggbox-type folded geometries, International Journal of Space Structures, 30, 2015, 99-110.

[10] Z. Chen, T. Wu, G. Nian, Y. Shan, X. Liang, H. Jiang, S. Qu, Ron Resch Origami Pattern Inspired Energy Absorption Structures, Journal of Applied Mechanics, 86, 2018, 011005-011005-011007.

[11] Z. Zhang, M.H. Litt, L. Zhu, K. Fuchi, A.S. Gillman, P.R. Buskohl, A Deployable Origami Structure Design for Packaging Cushioning (Preprint), in, Rutgers University New Brunswick United States, 2017.

[12] H. Fang, S.A. Chu, Y. Xia, K.W. Wang, Programmable Self-Locking Origami Mechanical Metamaterials, Adv Mater, 30, 2018, e1706311.

[13] Z. Zhai, Y. Wang, H. Jiang, Origami-inspired, on-demand deployable and collapsible mechanical metamaterials with tunable stiffness, Proceedings of the National Academy of Sciences, 115, 2018, 2032-2037.

[14] Z. Li, W. Chen, H. Hao, Crushing behaviours of folded kirigami structure with square dome shape, International Journal of Impact Engineering, 115, 2018, 94-105.

[15] Z. Li, W. Chen, H. Hao, Numerical study of open-top truncated pyramid folded structures with interconnected side walls against flatwise crushing, Thin-Walled Structures, 132, 2018, 537-548.

[16] Z. Li, W. Chen, H. Hao, Blast mitigation performance of cladding using Square Dome-shape Kirigami folded structure as core, International Journal of Mechanical Sciences, 145, 2018, 83-95.

[17] Z. Li, W. Chen, H. Hao, Blast resistant performance of cladding with folded open-top truncated pyramid structures as core, in: 7th International Meeting on Origami in Science, Mathematics, and Education, Oxford, UK, 2018.

[18] Z. Li, W. Chen, H. Hao, J. Cui, Y. Shi, Experimental study of multi-layer folded truncated structures under dynamic crushing, International Journal of Impact Engineering, 131, 2019, 111-122.

[19] G. Lu, T. Yu, Energy Absorption of Structures and Materials, Woodhead publishing limited, Cambridge England, 2003.

[20] M.F. Ashby, A. Evans, N.A. Fleck, L.J. Gibson, J.W. Hutchinson, H.N.G. Wadley, Metal foams: a design guide, Materials & Design, 23, 2002, 119.

[21] Y. Zhang, X. Xu, G. Sun, X. Lai, Q. Li, Nondeterministic optimization of tapered sandwich column for crashworthiness, Thin-Walled Structures, 122, 2018, 193-207.

[22] G. Sun, S. Li, Q. Liu, G. Li, Q. Li, Experimental study on crashworthiness of empty/aluminum foam/honeycomb-filled CFRP tubes, Composite Structures, 152, 2016, 969-993.

[23] W. Chen, T. Wierzbicki, Relative merits of single-cell, multi-cell and foam-filled thin-walled structures in energy absorption, Thin-Walled Structures, 39, 2001, 287-306.

[24] P.-B. Su, B. Han, M. Yang, Z.-H. Wei, Z.-Y. Zhao, Q.-C. Zhang, Q. Zhang, K.-K. Qin, T.J. Lu, Axial compressive collapse of ultralight corrugated sandwich cylindrical shells, Materials & Design, 160, 2018, 325-337.

[25] X. Zhang, G. Cheng, A comparative study of energy absorption characteristics of foam-filled and multi-cell square columns, International Journal of Impact Engineering, 34, 2007, 1739-1752.

[26] ASTM, E8M-04 Standard Test Methods for Tension Testing of Metallic Materials (Metric) 1, ASTM international, 2004.

[27] W. Chen, H. Hao, D. Hughes, Y. Shi, J. Cui, Z.-X. Li, Static and dynamic mechanical properties of expanded polystyrene, Materials & Design, 69, 2015, 170-180.

606 [28] F. Côté, V.S. Deshpande, N.A. Fleck, A.G. Evans, The out-of-plane compressive behavior
607 of metallic honeycombs, Materials Science and Engineering: A, 380, 2004, 272-280.

608 [29] Z. Ozdemir, E. Hernandez-Nava, A. Tyas, J.A. Warren, S.D. Fay, R. Goodall, I. Todd, H.
609 Askes, Energy absorption in lattice structures in dynamics: Experiments, International Journal
610 of Impact Engineering, 89, 2016, 49-61.

611 [30] M. Zupan, C. Chen, N.A. Fleck, The plastic collapse and energy absorption capacity of
612 egg-box panels, International Journal of Mechanical Sciences, 45, 2003, 851-871.

613 [31] E. Avallone, T. Baumeister, Mark's standard handbook for mechanical engineers,
614 McGraw-Hill, 2017.

615 [32] T. Yu, X. Qiu, Introduction to impact dynamics, John Wiley & Sons, 2018.

616 [33] Z. Xue, J.W. Hutchinson, Crush dynamics of square honeycomb sandwich cores,
617 International Journal for Numerical Methods in Engineering, 65, 2006, 2221-2245.

618